

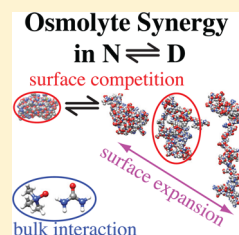
# Synergy in Protein–Osmolyte Mixtures

Jörg Rösgen\*

Department of Biochemistry and Molecular Biology, Penn State University College of Medicine, Hershey, Pennsylvania 17033, United States

**S** Supporting Information

**ABSTRACT:** Virtually all taxa use osmolytes to protect cells against biochemical stress. Osmolytes often occur in mixtures, such as the classical combination of urea with TMAO (trimethylamine *N*-oxide) in cartilaginous fish or the cocktail of at least six different osmolytes in the kidney. The concentration patterns of osmolyte mixtures found *in vivo* make it likely that synergy between them plays an important role. Using statistical mechanical *n*-component Kirkwood–Buff theory, we show from first principles that synergy in protein–osmolyte systems can arise from two separable sources: (1) mutual alteration of protein surface solvation and (2) effects mediated through bulk osmolyte chemical activities. We illustrate both effects in a four-component system with the experimental example of the unfolding of a notch ankyrin domain in urea–TMAO mixtures, which make urea a less effective denaturant and TMAO a more effective stabilizer. Protein surface effects are primarily responsible for this synergy. The specific patterns of surface solvation point to denatured state expansion as the main factor, as opposed to direct competition.



## INTRODUCTION

Small organic osmolytes are molecules that virtually all organisms use to counter cellular stresses.<sup>1</sup> Many of these molecules are known to have a profound impact on biological macromolecules<sup>2–5</sup> and are thus of broad research interest. A debate has been going on for decades about the mechanism of the action of *individual* types of osmolytes.<sup>5–44</sup> However, nature often uses mixtures of several of them.<sup>45</sup> For example, a mixture of five osmolytes counters the combined deleterious effects of high concentrations of salt and urea in mammalian kidneys.<sup>46</sup> Osmolyte cocktails may be necessary for several reasons. The use of a diverse set of osmolytes permits protection of multiple classes of biomolecules from deleterious effects of urea.<sup>47</sup> Alternatively, synergy between osmolytes may enhance their efficacy in mixtures. Indeed, such synergy has been observed *in vitro*.<sup>48–50</sup> Also, the concentrations of renal osmolytes *in vivo* do not all seem to scale linearly with the abundance of stressor molecules,<sup>51</sup> again pointing toward synergy as a factor to be considered.

Here, we investigate what solvation patterns can lead to synergy between osmolytes. General equations are derived, which are valid beyond osmolytes and proteins. As an illustration we use experimental data on several proteins to determine the cause for synergy in various cases. We start out with a brief discussion of the thermodynamic basis of osmolyte action—the concept of preferential interaction.

## PREFERENTIAL INTERACTION

Water and osmolyte act as low-affinity ligands that compete for interaction sites at the macromolecular surface.<sup>11</sup> Osmolyte concentrations in nature can be quite high, reaching up to several molar.<sup>52</sup> Under such conditions the cosolute concentration(s) substantially affect the water concentration. As a result, the thermodynamic binding stoichiometry  $N_{ik}$  of component *i* to component *k* is modified by the binding

stoichiometry  $N_{1k}$  of the competing water. This thermodynamic stoichiometry has been termed preferential interaction parameter  $\Gamma_{ik}$ <sup>9</sup>

$$\Gamma_{ik} = N_{ik} - \frac{c_i}{c_1} N_{1k} \quad (1)$$

where  $c_i$  are molarities and the index 1 stands for water.

The concept of preferential solvation has a solid physical underpinning in Kirkwood–Buff theory.<sup>53</sup> Radial distribution functions,  $g_{ik}$ , represent the concentration profile of particles of type *i* around those of type *k* relative to the bulk concentration. Integrating  $g_{ik}$  gives the relative excess or deficit of particle type *i* around particle type *k* (and vice versa):

$$\mathcal{G}_{ik} = \int (g_{ik} - 1) dv \quad (2)$$

The preferential interaction parameter defined in eq 1 can be rewritten in terms of the Kirkwood–Buff integrals defined in eq 2

$$\Gamma_{ik} = (\mathcal{G}_{ik} - \mathcal{G}_{1k})c_i \quad (3)$$

because  $N_{ik} = c_i \mathcal{G}_{ik}$ .<sup>54</sup> This equation provides a more generalized outlook. The original idea for preferential interaction parameters (eq 1) allows only for positive stoichiometries. The Kirkwood–Buff integrals  $\mathcal{G}_{ik}$ , however, can be negative because of the mutual volume exclusion of the molecules.

Beyond eq 1, there are many definitions for various types of preferential interaction parameters<sup>55</sup> that are motivated by particular experimental methods and their specific constraints.<sup>28,56,57</sup> In the following we will use the definition of

**Received:** November 6, 2014

**Revised:** December 8, 2014

**Published:** December 9, 2014

eqs 1 and 3, which is based on the intuitive meaning of “preferential interaction” as the difference in the interaction of a substance  $k$  with component  $i$  and with water.<sup>9</sup>

## ■ HOW TO QUANTIFY SYNERGY

Osmolytes are known to stabilize or destabilize proteins, i.e., to fold<sup>3</sup> or unfold<sup>2</sup> them. The slope of the protein stability with the molar osmolyte concentration  $c_O$  is the  $m$ -value,<sup>2</sup> which relates to the ratio of molar activity coefficients  $\gamma_D/\gamma_N$  of the pure native (N) and denatured (D) states by<sup>58</sup>

$$\frac{m_O}{RT} = -\left(\frac{\partial \ln K}{\partial c_O}\right) = \left(\frac{\partial \ln(\gamma_D/\gamma_N)}{\partial c_O}\right) \quad (4)$$

where  $K = c_D/c_N$  is the equilibrium constant of the protein conformational transition,  $R$  is the gas constant,  $T$  is the temperature, and  $c_D$  and  $c_N$  are the concentrations of the D and N states, respectively. The  $m$ -values appear to be constants when looking at individual natural osmolytes.<sup>2,15,21,59–63</sup> Nonconstant  $m$ -values have been reported in thermal unfolding,<sup>64</sup> which could be an artifact of irreversible precipitation of the D state at high osmolyte concentration.<sup>65</sup>  $m$ -value constancy may<sup>30,63</sup> or may not<sup>48–50</sup> hold for mixtures of osmolytes, and we will take a closer look at this issue here.

When the  $m$ -value of one osmolyte is independent of the presence of another osmolyte, they act additively. If two osmolytes affect each other (show synergy or antagonism), both  $m$ -values must change in the same direction for symmetry reasons (Maxwell relations).<sup>50,63</sup> For simplicity, we will not differentiate between synergy and antagonism in the following.

## ■ METHODS

**Curve Fitting.** The protein stability data were fit using a stability equation that depends on both osmolytes' concentrations:<sup>50</sup>

$$-\log K = \frac{m_U}{RT}(c_U - c_m) + \frac{m_T}{RT}c_T + \frac{m_{UT}}{RT}(c_U - c_m)c_T \quad (5)$$

The  $m$ -values for urea ( $m_U + m_{UT}c_T$ ) and trimethylamine  $N$ -oxide (TMAO) ( $m_T + m_{UT}c_U$ ) depend mutually on each other's concentration. The populations of the N state,  $1/(1 + K)$ , and D state,  $K/(1 + K)$ , are weighted by the respective state's signal to obtain the fits shown in Figure 1A, as explained previously.<sup>50</sup>

**Simulations.** Markov chain Metropolis Monte Carlo simulations using the ABSINTH implicit solvation model<sup>66</sup> and the OPLS-AA/L charge set were performed in the canonical ensemble ( $T = 288$  K for Nank4–7\*, and  $T = 298$  K otherwise) with a properly adjusted dielectric constant.<sup>67</sup> Each sequence was enclosed in a spherical droplet of 450 Å radius. We modeled explicitly represented  $\text{Na}^+$  and  $\text{Cl}^-$  ions sufficient to neutralize the net polypeptide charge. The systems were equilibrated for 30 million steps, and data were collected for at least 70 million steps. Simulations were repeated at least four times.

Solvent excluded volumes were calculated using MOLMOL.<sup>68</sup> Such an excluded volume approach can be used for quantifying the thermodynamic effect of inert additives (governed by hard-core repulsion) at dilute concentrations.<sup>69</sup> TMAO exists in solution as a strong dihydrate that is approximately spherical.<sup>40</sup> The van der Waals volume of TMAO<sup>34</sup> plus two water molecules gives an effective spherical radius of only 2.89 Å for the dihydrate. Replacing one or both

hydration waters with urea results in 3.24 and 3.54 Å, respectively. The exclusion of TMAO in the presence of urea was calculated, weighing the results obtained for each of these radii by the corresponding population of that species.<sup>40</sup>

## ■ RESULTS AND DISCUSSION

**Synergy in Protein–Osmolyte Systems.** *Experimental Observations.* There are a few examples that show the thermodynamics of proteins in osmolyte mixtures, and synergy is found to exist. TMAO has been shown to lessen the  $m$ -value of guanidinium chloride (gdmCl) for a thermophilic ribonuclease HII by a remarkable 25% per molar concentration of TMAO.<sup>48</sup> Note that this effect goes beyond the trivially expected stabilization of the protein by TMAO, which leads to the requirement to add more gdmCl to reach the transition midpoint concentration  $c_{1/2}$ . TMAO decreases the efficiency of gdmCl as a denaturant on top of such simple additivity. An example of synergy between two protein stabilizers is that between glucose and fructose. The thermal stability of ribonuclease A in mixtures of these two osmolytes is less than would be expected from additive contributions of the individual sugars, as seen by comparing the transition midpoint temperatures  $T_{1/2}$ .<sup>49</sup>

The causes of such synergistic effects cannot be easily identified without knowledge of some additional thermodynamic parameters. Therefore, we focus on an example for which all essential data are available, viz., the effect of mixtures of TMAO with urea<sup>40</sup> on the notch ankyrin domains Nank1–7\* and Nank4–7\* and on barnase.<sup>63</sup> Figure 1A–C shows spectroscopic traces of the three proteins as a function of the osmolyte concentration.<sup>63</sup> A fit to eq 5 reveals that the  $m$ -values for urea and TMAO depend on each other to different degrees for the three proteins, as seen in Table 1. To be able to compare the synergies ( $m_{UT}$ ) with each other, we divide  $m_{UT}$  by

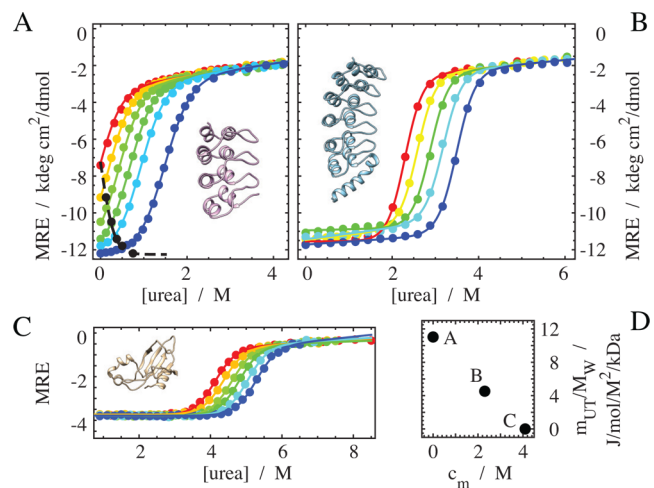


**Figure 1.** Effect of urea–TMAO mixtures on three proteins. Urea-induced unfolding at variable TMAO concentrations of Nank4–7\*, Nank1–7\*, and barnase (A–C). Molar TMAO concentrations (from left to right) are 0, 1/8, 1/4, 3/8, 1/2, and 3/4 (A), 0 to 1/2 (B), and 0 to 1 (C). Dashed line: TMAO-induced folding of Nank4–7\*. The points are experimental data<sup>63</sup> and the lines a global fit to eq 5. The insets show native structures (1mb (PDB) and full-length/truncated 1ot8 (PDB)) drawn with Chimera.<sup>70</sup> (D) Dependence of the  $M_w$ -normalized synergy between urea and TMAO on  $c_m$  of the urea-induced unfolding. The letters indicate from which panel the point is taken.

Table 1. Fitting Parameters for Figure 1

	Nank4–7*	Nank1–7*	barnase
$m_U/\text{kJ}/(\text{mol M})$	9.1	11.7	8.0
$m_T/\text{kJ}/(\text{mol M})$	-16.2	-26.7	-9.3
$m_{UT}/\text{kJ}/(\text{mol M}^2)$	-1.5	-1.0	-0.1
$c_m/\text{M}$	-0.1	2.3	4.1
$M_w/\text{kDa}$	9.1	11	8

the proteins' molecular weight, because  $m$ -values scale with the size of the proteins.<sup>36</sup> Figure 1D shows that the synergies of the three proteins show a concentration pattern when plotted together. At 0 M urea (Nank4–7\*) the synergy starts at a substantial level corresponding to about a 25% change of the  $m$ -value for urea between 0 and 1.5 M TMAO. Interestingly, the synergy vanishes toward 4 M urea (barnase). This could indicate involvement of denatured state expansion/contraction, because at elevated urea the denatured proteins may converge toward a maximally extended state. Then  $m_{UT}$  would be sampled in a region without expansion/contraction when the transition is observed at a higher urea concentration. We will discuss this idea further below.

There are several possible explanations for the variable degrees of synergy, including a mutual influence of the chemical activities of the various bulk solution species on each other,<sup>40</sup> enhanced exclusion of TMAO from the protein surface by a layer of urea that builds up as denaturant is added,<sup>40</sup> or a change in D state excluded volume<sup>20</sup> by chain expansion/contraction with osmolyte concentration.<sup>30,35</sup> In the following sections we will first analyze where such synergy can come from in principle. Then we will investigate the given data to assess how the synergy arises in these specific systems.

**Calculation of  $m$ -Values and Solvation Parameters.** The  $m$ -value can be expressed in two alternative ways which are based on either preferential interaction parameters of solution components with protein,  $\Gamma_{iP}$ , or the relative excess/deficit of each solution component around the protein,  $\mathcal{G}_{iP}$ . As shown in the Supporting Information, the equation is

$$-\frac{m_j}{RT} = \sum_{i \neq 1, P} \gamma_{ij} \Delta \Gamma_{iP} = \sum_{i \neq P} \gamma_{ij} c_i \Delta \mathcal{G}_{iP} \quad (6)$$

for small protein concentration, where P stands for protein,  $m_j$  is the  $m$ -value for component  $j$ , and  $\Delta$  indicates differences between the two protein states, and we define

$$\gamma_{ij} = \left( \frac{\partial \ln a_i}{\partial c_j} \right)_{c_k \neq j} \quad (7)$$

where  $a_i$  is the chemical activity of component  $i$ . Note that the sum excludes water (component 1) in one case and includes it in the other.

Equation 6 is surprisingly simple. It reveals that the  $m$ -value of a protein transition with respect to component  $j$  depends on two major factors: First,  $m$ -values depend on the change in protein solvation upon unfolding,  $\Delta \Gamma_{iP}$  or  $\Delta \mathcal{G}_{iP}$ , with respect to each of the solution components. This factor quantifies the direct interaction of the solution with the protein, and it depends on both the type and the amount of solvent-exposed surface. The usual focus is on the type of surface area.<sup>15,71</sup> However, osmolyte-dependent changes in D state compaction can affect  $m$ -values through alterations in the amount of exposed area,<sup>35</sup> and this effect seems to play a role in osmolyte

synergy as well (see below). Second,  $m$ -values depend on the degree to which each component's activity coefficient changes with the concentration of the variable component  $j$ ,  $\gamma_{ij}$ . This factor is rooted in the interactions in the bulk solution, where the added component can alter how much other components are worth in terms of their chemical activity. Note that synergy can thus occur even if the osmolytes act independently of each other at the protein surface, because with increasing concentration of osmolyte type  $i$  the term  $\gamma_{ij} c_i \Delta \mathcal{G}_{iP}$  for that osmolyte is dialed in, thereby modifying  $m_j$  (eq 6).

On the basis of eq 6, there are only three extreme cases that could lead to an absence of synergy between two osmolytes: (1) Their chemical activities are independent of each other ( $\gamma_{ij} = 0$  for  $i \neq j$ ). (2) The change in solvation upon unfolding ( $\Delta \mathcal{G}_{iP}$ ) is zero for both osmolytes; i.e., neither of them affects the protein anyway. (3) Finally, there is a fortuitous canceling of effects. Obviously, none of these hold in general. Then synergy may be expected to be the norm, rather than an exception. If synergy is the norm, why is it then not normally reported? There are only a few studies of the effects of mixtures of osmolytes on proteins. Also, it can be difficult to detect synergy with conventional data analysis methods, even if the synergy is significant.<sup>50</sup>

To calculate the individual terms in eq 6, we need an equation for  $\Delta \mathcal{G}_{iP}$ . The other components of eq 6 have been published previously for aqueous urea/TMAO.<sup>40</sup> In the Supporting Information we show exact equations for  $\mathcal{G}_{kP}$  and  $\Gamma_{kP}$  (eqs S10 and S11, Supporting Information). For better readability, we use the following three convenient simplifications: The compressibility is negligibly small for our purposes,<sup>72</sup> the change in volume upon unfolding,  $\Delta \bar{v}_P$ , is small as well (on the order of less than  $\pm 0.1 \text{ L/mol}^{73-76}$ ), and we are dealing with dilute protein. In vitro protein concentrations are usually low. Typical in vivo conditions involve an abundance of proteins, many of which are present at very low concentrations. Therefore, despite high total protein, most individual protein types are dilute. The change in protein solvation upon unfolding,  $\Delta \mathcal{G}_{kP}$ , is given by the difference of eq S10 between the N and D states. We obtain

$$\Delta \mathcal{G}_{kP} = -\frac{m_k}{RT} - \sum_{i \neq 1, P} \frac{m_i}{RT} c_i \mathcal{G}_{ki} \quad (8)$$

and

$$\Delta \Gamma_{kP} = -\frac{m_k}{RT} c_k - \sum_{i \neq 1, P} \frac{m_i}{RT} c_i \Gamma_{ki} \quad (9)$$

where we used  $m_k = RT \Delta \gamma_{Pk}$  (eq 4).

There is no  $m_1$  value (cf. eq S23, Supporting Information), and thus, the hydration of the protein  $\Delta \mathcal{G}_{1P}$  needs to be calculated from the other  $\Delta \mathcal{G}_{kP}$  through eq S6 (Supporting Information):

$$\Delta \mathcal{G}_{1P} = -\sum_{i > 1} \frac{c_i \bar{v}_i}{c_1 \bar{v}_1} \Delta \mathcal{G}_{iP} \quad (10)$$

**Analysis of Protein Solvation in Urea–TMAO Mixtures. General Overview and Water Contributions.** To calculate the solvation behavior around the protein from eqs 8 and 10, we use the experimental  $m$ -values from Table 1 along with published activity coefficients.<sup>40</sup> The resulting curves are shown in Figure 2. We first note that  $\Delta \mathcal{G}_{UP}$  is positive, i.e. urea becomes more accumulated at the protein surface upon unfolding. Conversely, TMAO becomes more depleted

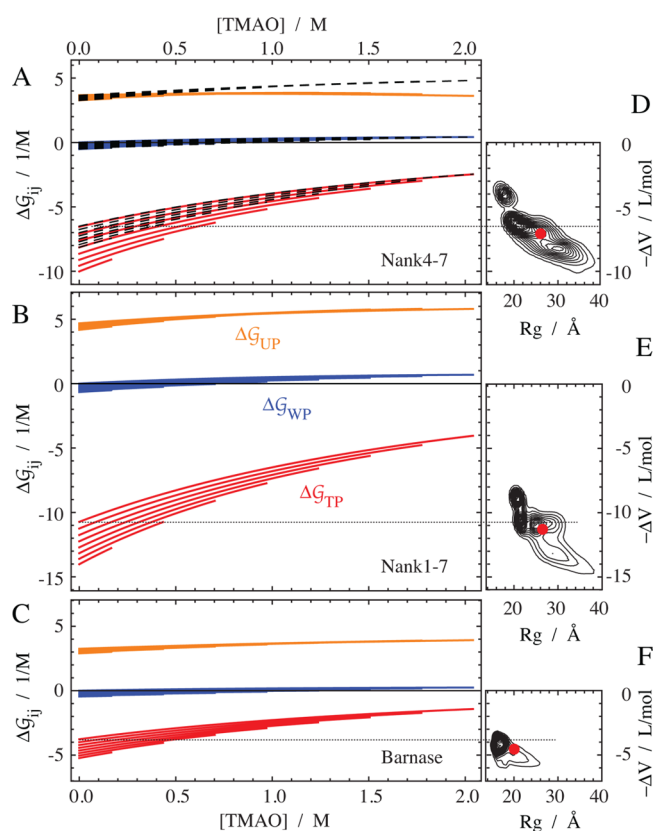


**Figure 2.** Solvation change of Nank4–7\* (A), Nank1–7\* (B), and barnase (C) upon unfolding with respect to protein solvation by urea ( $\Delta G_{UP}$ , orange), TMAO ( $\Delta G_{TP}$ , red), and water ( $\Delta G_{WP}$ , blue). The curves were calculated using eqs 8 and 10. Each group of curves represents increasing urea concentration from 0 to 3.5 M in 0.5 M steps (long to short curves). The dashed lines in panel A indicate a solvation pattern that would result in a lack of synergy. Panels D–F show an estimate for the change of TMAO excluded volume upon unfolding vs the radius of gyration of the D state. Distributions/averages for TMAO dihydrate are shown in black/red.

(negative  $\Delta G_{TP}$ ). The hydration change ( $\Delta G_{WP}$ ) is very small. Thus, the water contributes comparatively little to the change in preferential interaction (eq 3), as pointed out previously.<sup>29</sup>

From these solvation data it is also possible to calculate all contributions to the  $m$ -values. The right-hand side of eq 6 sums three terms in aqueous solutions of urea and TMAO. These terms are shown in Figure 3 for our three proteins. The general observation is that the primary contribution to the urea  $m_U$ -values comes from the urea term and that to the TMAO  $m_T$ -values from the TMAO term. Only upon the addition of osmolyte are the water term and the respective other osmolytes' terms dialed in to some degree.

The bulk solution contribution to each of the three solvation terms in eq 6 is shown in Figure 3G. Urea and TMAO enhance each other's chemical activity (positive  $\gamma_{UT}$  and  $\gamma_{TU}$ ). In the absence of any further consideration, one may therefore be tempted to assume that urea and TMAO enhance each other's effect on proteins; i.e., urea becomes a stronger denaturant and TMAO a stronger stabilizer. However, this cannot be, because opposite slopes of  $m_U$  and  $m_T$  would violate the Maxwell relations mentioned above. Thus, it is obvious that a more careful analysis of the solvation is necessary.

In Figure 3A–F the water term,  $\gamma_{Wi}^c \Delta G_{WP}$ , always becomes more positive when urea is added and more negative when

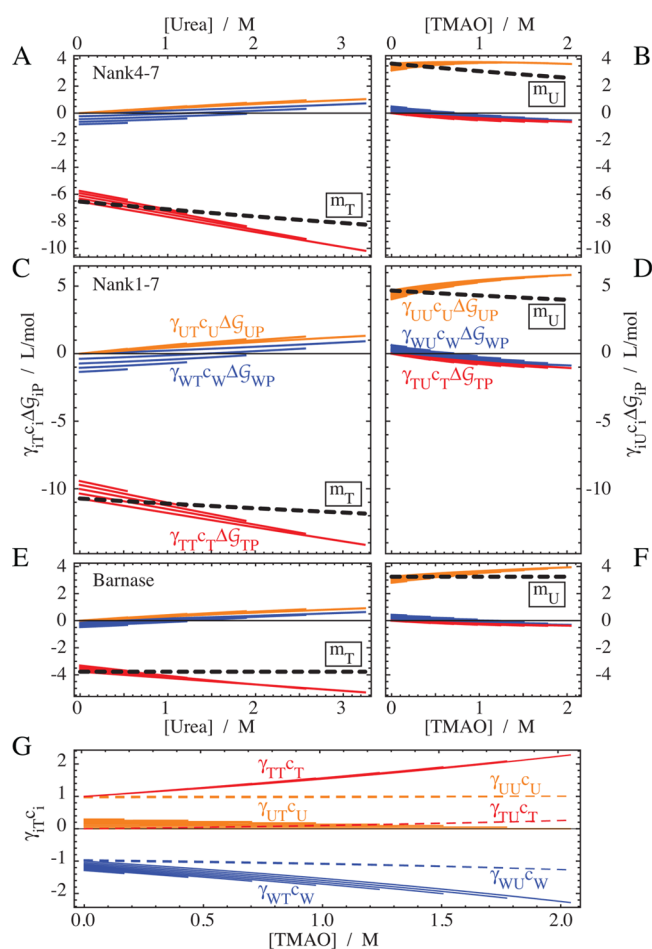


**Figure 3.** Contributions to the  $m$ -values of Nank4–7\* (A, B), Nank1–7\* (C, D), and barnase (E, F) with respect to urea (right) and TMAO (left). The  $m$ -values are given by the bold dashed line and the various additive terms in eq 6 by orange (urea), blue (water), and red (TMAO) lines. Each group of lines of decreasing length represent increasing concentrations of the other respective osmolyte from 0 to 3.3 M (urea) or 2 M (TMAO). (G) Bulk solution terms: Dependence of the chemical activities of urea (U), TMAO (T), and water (W) on the TMAO concentration<sup>40</sup> ( $\gamma_{ij}$  are defined in eq 7). Note that the solid lines add up to zero, as well as the dashed lines (Gibbs–Duhem relation).

TMAO is added. That is, the water enhances the effect of the added osmolyte. The cause for this phenomenon is classical preferential binding/exclusion, as follows. In Figure 2A–C we see that addition of TMAO leads to preferential hydration (positive  $\Delta G_{WP}$ ), whereas addition of urea (going from the longer to the shorter lines) leads to preferential exclusion of water (negative  $\Delta G_{WP}$ ). This makes sense, because accumulation of urea should mean that water becomes excluded and exclusion of TMAO that water is accumulated. Therefore,  $\Delta G_{WP}$  has the opposite trend compared to both  $\Delta G_{UP}$  and  $\Delta G_{TP}$ , but  $\gamma_{Wi}^c \Delta G_{WP}$  is negative (water gets diluted upon osmolyte addition), so that the water term,  $\gamma_{Wi}^c \Delta G_{WP}$ , always tracks with the effect of the osmolyte that is added.

**Urea–Protein Solvation.** The change in protein solvation by urea upon unfolding,  $\Delta G_{UP}$ , is shown in Figure 2A–C as a group of orange lines representing one urea concentration each.  $\Delta G_{UP}$  depends little on the concentrations of urea and TMAO. This makes sense, because accumulated (urea) and depleted (TMAO) osmolytes should not interfere with each other at the

protein surface.<sup>30,77</sup> Note, however, that  $\Delta\mathcal{G}_{UP}$  slightly increases as a function of TMAO when no or little synergy is observed (Figure 2B,C). This can be illustrated also by setting  $m_{UT}$  to 0 (Figure 2A, dashed lines), which results in a clear upward slope for  $\Delta\mathcal{G}_{UP}$ . It is known that TMAO compacts the D state of proteins<sup>78</sup> including Nank4–7\*,<sup>79</sup> which should lead to a reduced accessibility to urea and hence a smaller urea accumulation and a smaller  $m$ -value.<sup>35</sup> Thus, the presence of compaction diminishes the observed increase in  $\Delta\mathcal{G}_{UP}$ . One may conclude then that in the case of Nank4–7\* (panel A) there is more compaction of the D state ensemble with TMAO, compared to Nank1–7\* (panel B) and barnase (panel C), because Nank4–7\* shows the least increase of  $\Delta\mathcal{G}_{UP}$ . Such a conclusion is also consistent with the observed patterns in the protein–TMAO solvation  $\Delta\mathcal{G}_{TP}$ .

In the absence of synergy  $\Delta\mathcal{G}_{UP}$  increases slightly as a function of TMAO, and the question is why it increases at all. Even if competition between urea and TMAO occurred at the protein surface, it would lead to the opposite effect of displacing urea, and not accumulating more of it. Also changes in the total surface area would lead to the opposite effect, as discussed in the previous paragraph. What is left as a reason for the increase in  $\Delta\mathcal{G}_{UP}$  are bulk solution effects. As TMAO is added, the chemical activity of urea increases.<sup>40</sup> As a consequence, more urea is driven to the protein surface than normally expected at the same nominal urea concentration. Therefore,  $\Delta\mathcal{G}_{UP}$  increases with added TMAO.

**TMAO–Protein Solvation.** Figure 2 shows the change in protein solvation by TMAO,  $\Delta\mathcal{G}_{TP}$ , as red lines. Comparing the solvation of the proteins, there are both similarities and differences. A similarity is that for all three proteins  $\Delta\mathcal{G}_{TP}$  changes to a third of its value between 0 and 2 M TMAO in the absence of urea. Such a pattern is expected for an entity such as TMAO that is dominated by hard-core repulsion.<sup>40</sup> A difference between the proteins is that for Nank4–7\*  $\Delta\mathcal{G}_{TP}$  becomes more negative by over half its value from 0 to 3.5 M urea in the limit of 0 M TMAO, whereas it is only about one-third for the other two proteins. We previously postulated that TMAO should become spaced further from the protein in the presence of urea, because the effective size of TMAO increases as it becomes solvated by urea.<sup>40</sup> This postulate is clearly consistent with the current observation, but cannot be the whole truth since the magnitude of the increase in TMAO exclusion is dependent on the type of protein, pointing again to D state contraction/expansion. As TMAO can contract D state ensembles of proteins,<sup>78,79</sup> urea is expected to expand them in general.<sup>35,80–84</sup> Expansion may not hold for all proteins,<sup>85</sup> but is specifically known to happen in the case of Nank4–7\*.<sup>79</sup> A more extended D state results in more exclusion of TMAO, which is consistent with the observed enhancement of  $\Delta\mathcal{G}_{TP}$  with added urea. For Nank4–7\*, this change in protein–TMAO solvation is larger than for the other proteins, so the D state of Nank4–7\* likely expands most, just as it contracts most with TMAO as discussed above.

Both D state expansion and increased spacing away of TMAO from the protein surface by urea could thus contribute to the observed  $\Delta\mathcal{G}_{TP}$ . Estimating the contribution of the latter effect is comparably straightforward when considering only hard-core repulsion. TMAO exists in solution as a strong dihydrate that is approximately spherical, and the water can be replaced by urea to increase the effective spherical radius.<sup>40</sup> The spherical dimensions of TMAO capture its own solvation in aqueous urea fairly well,<sup>40</sup> and simulations indicate that TMAO

likely interacts with proteins only in a manner mediated by the solvent,<sup>86</sup> as expected for mandatory hydration/urea solvation. In the limit of ideal dilution (0 M osmolyte and protein), the  $\Delta\mathcal{G}_{PT}$  is simply given by the negative of the change in contact volume, when only hard-core repulsion plays a role. The calculation of the N state contact volume is straightforward. To get an estimate for the D state, we used an ensemble generated through Monte Carlo simulation. The difference between the D and N state exclusion volumes is shown in Figure 2D–F. The average exclusion volume,  $-\Delta V$ , for the dihydrate (red dots) is close to the corresponding values in panels A–C (0 M osmolyte), as indicated by the dotted line. Also the radius of gyration ( $R_g$ ) of about 26 Å for Nank4–7\* that we find at 15 °C makes sense, given that the experimental hydrodynamic radius is 29.5 Å at 55 °C.<sup>79</sup> Therefore, the generated ensemble appears to generally make sense, and plain volume exclusion of TMAO from the protein is a reasonable assumption.

On the basis of the simulated D states, we are now in the position to estimate the contribution of TMAO becoming more excluded from the protein by urea functioning as a spacer (in the absence of D state expansion). The result is essentially independent of the specifics of the ensemble. We obtain about 0.5–1 L/mol enhancement of  $\Delta\mathcal{G}_{TP}$  between 0 and 3.5 M urea using any of the simulated D state structures. The actual urea dependence of  $\Delta\mathcal{G}_{TP}$  always far exceeds this estimate. This suggests that our original postulate of urea acting as spacers is not sufficient to explain the solvation of proteins by TMAO in aqueous urea and that D state expansion needs to be considered. Moreover, previous simulations indicated that urea and TMAO likely do not interfere with each other at the protein surface.<sup>77</sup> Then synergy between urea and TMAO is mediated mostly by an increase in total area through changes in the D state ensemble, rather than either bulk solution or surface competition effects.

Our estimated D state ensembles provide additional qualitative information on the question of why the D state of Nank4–7\* may be more responsive to osmolytes than the other proteins. The ensemble sampled for Nank4–7\* (Figure 2D) not only covers a broader range than the ensembles sampled for Nank1–7\* and barnase (Figure 2E,F), but also has a larger variance in  $\Delta V$ , which likely enables Nank4–7\* to be much more responsive to changes in solution conditions that favor contraction or expansion.

**Generalization to Specific Binding.** We have only discussed addition of two osmolytes so far, but our equations can be easily extended to any number of interacting components, including specific binding partners. As an illustration, we consider a single binding site on a protein, which is occupied by ligands whose number is given by

$$N_{LP} = \frac{c_L K_b}{1 + c_L K_b} \quad (11)$$

where  $c_L$  is the ligand concentration and  $K_b$  the binding constant. Then because  $N_{ik} = c_i \mathcal{G}_{ib}$ ,<sup>54</sup> we have

$$\mathcal{G}_{PL} = \frac{K_b}{1 + c_L K_b} \quad (12)$$

With such specific interactions, stronger synergies may be expected even at low ligand concentrations, because osmolytes can have significant interactions with free ligands.<sup>87–89</sup> The synergy then comes solely from the  $\gamma_{LO}$  term in eq 6. Allosteric

effects are an example of the other extreme of synergy solely based on surface effects ( $\Delta G_{ij}$ ).

## CONCLUSION

We have presented rigorous, yet concise equations that capture the thermodynamic synergy between any number of solution components. These equations show how surface solvation and bulk solution interactions can lead to synergies. Using three example proteins, we illustrated the extent to which these various interactions contribute to synergy. The protein surface component turns out to be the primary factor. The actual interactions of the osmolytes with the surface are not very dependent upon each other, but it is the change in D state exposed area that appears to be mainly responsible for synergy in protein conformational changes.

## ASSOCIATED CONTENT

### Supporting Information

Fundamental Kirkwood–Buff equations, derivation of eqs 6 and 8, and base transform to the molar scale. This material is available free of charge via the Internet at <http://pubs.acs.org/>.

## AUTHOR INFORMATION

### Corresponding Author

\*E-mail: [Jorg.Rosgen@psu.edu](mailto:Jorg.Rosgen@psu.edu).

### Notes

The authors declare no competing financial interest.

## ACKNOWLEDGMENTS

Cecilia Mello and Doug Barrick kindly provided the data in Figure 1 for reanalysis. We thank Montgomery Pettitt, Wayne Bolen, and Prem Sinha for helpful discussions. The research reported in this paper was supported by NIH/NIGMS Grant GM049760.

## REFERENCES

- (1) Yancey, P.; Clark, M.; Hand, S.; Bowlus, R.; Somero, G. Living with water stress: Evolution of osmolyte systems. *Science* **1982**, *217*, 1214–1222.
- (2) Greene, R. J.; Pace, C. Urea and guanidine hydrochloride denaturation of ribonuclease, lysozyme,  $\alpha$ -chymotrypsin, and  $\beta$ -lactoglobulin. *J. Biol. Chem.* **1974**, *249*, 5388–5393.
- (3) Baskakov, I.; Bolen, D. W. Forcing thermodynamically unfolded proteins to fold. *J. Biol. Chem.* **1998**, *273*, 4831–4834.
- (4) Courtenay, E.; Capp, M.; Anderson, C.; Record, M. J. Vapor pressure osmometry studies of osmolyte-protein interactions: Implications for the action of osmoprotectants in vivo and for the interpretation of “osmotic stress” experiments in vitro. *Biochemistry* **2000**, *39*, 4455–4471.
- (5) Auton, M.; Bolen, D. W. Predicting the energetics of osmolyte-induced protein folding/unfolding. *Proc. Natl. Acad. Sci. U.S.A.* **2005**, *102*, 15065–15068.
- (6) Schellman, J. A. The stability of hydrogen-bonded peptide structures in aqueous solution. *C. R. Trav. Lab. Carlsberg, Ser. Chim.* **1955**, *29*, 230–259.
- (7) Kauzmann, W. Some factors in the interpretation of protein denaturation. *Adv. Protein Chem.* **1959**, *14*, 1–63.
- (8) Nozaki, Y.; Tanford, C. The solubility of amino acids and related compounds in aqueous urea solutions. *J. Biol. Chem.* **1963**, *238*, 4074–4081.
- (9) Tanford, C. Extension of the theory of linked functions to incorporate the effects of protein hydration. *J. Mol. Biol.* **1969**, *39*, 539–544.
- (10) Tanford, C. Protein denaturation. C. Theoretical models for the mechanism of denaturation. *Adv. Protein Chem.* **1970**, *24*, 1–95.
- (11) Schellman, J. The thermodynamics of solvent exchange. *Biopolymers* **1994**, *34*, 1015–1026.
- (12) Wallqvist, A.; Covell, D. G.; Thirumalai, D. Hydrophobic interactions in aqueous urea solutions with implications for the mechanism of protein denaturation. *J. Am. Chem. Soc.* **1998**, *120*, 427–428.
- (13) Timasheff, S. N. In disperse solution, “osmotic stress” is a restricted case of preferential interactions. *Proc. Natl. Acad. Sci. U.S.A.* **1998**, *95*, 7363–7367.
- (14) Parsegian, V.; Rand, R.; Rau, D. Osmotic stress, crowding, preferential hydration, and binding: A comparison of perspectives. *Proc. Natl. Acad. Sci. U.S.A.* **2000**, *97*, 3987–3992.
- (15) Courtenay, E.; Capp, M.; Saecker, R.; Record, M. J. Thermodynamic analysis of interactions between denaturants and protein surface exposed on unfolding: Interpretation of urea and guanidinium chloride *m*-values and their correlation with changes in accessible surface area (asa) using preferential interaction coefficients and the local-bulk domain model. *Proteins* **2000**, Suppl. 4, 72–85.
- (16) Kazmirski, S.; Wong, K.; Freund, S.; Tan, Y.; Fersht, A.; Daggett, V. Protein folding from a highly disordered denatured state: The folding pathway of chymotrypsin inhibitor 2 at atomic resolution. *Proc. Natl. Acad. Sci. U.S.A.* **2001**, *98*, 4349–4354.
- (17) Schellman, J. Fifty years of solvent denaturation. *Biophys. Chem.* **2002**, *96*, 91–101.
- (18) Chitra, R.; Smith, P. E. Molecular association in solution: A Kirkwood–Buff analysis of sodium chloride, ammonium sulfate, guanidinium chloride, urea, and 2,2,2-trifluoroethanol in water. *J. Phys. Chem. B* **2002**, *106*, 1491–1500.
- (19) Bennion, B.; Daggett, V. The molecular basis for the chemical denaturation of proteins by urea. *Proc. Natl. Acad. Sci. U.S.A.* **2003**, *100*, 5142–5147.
- (20) Schellman, J. Protein stability in mixed solvents: A balance of contact interaction and excluded volume. *Biophys. J.* **2003**, *85*, 108–125.
- (21) Felitsky, D.; Record, M. J. Application of the local-bulk partitioning and competitive binding models to interpret preferential interactions of glycine betaine and urea with protein surface. *Biochemistry* **2004**, *43*, 9276–9288.
- (22) Shimizu, S. Estimating hydration changes upon biomolecular reactions from osmotic stress, high pressure, and preferential hydration experiments. *Proc. Natl. Acad. Sci. U.S.A.* **2004**, *101*, 1195–1199.
- (23) Shimizu, S.; Boon, C. The Kirkwood–Buff theory and the effect of cosolvents on biochemical reactions. *J. Chem. Phys.* **2004**, *121*, 9147–9155.
- (24) Rösgen, J.; Pettitt, B. M.; Bolen, D. W. Protein folding, stability, and solvation structure in osmolyte solutions. *Biophys. J.* **2005**, *89*, 2988–2997.
- (25) Athawale, M. V.; Dordick, J. S.; Garde, S. Osmolyte trimethylamine-*N*-oxide does not affect the strength of hydrophobic interactions: Origin of osmolyte compatibility. *Biophys. J.* **2005**, *89*, 858–866.
- (26) Auton, M.; Ferreon, A. C.; Bolen, D. W. Metrics that differentiate the origins of osmolyte effects on protein stability: A test of the surface tension proposal. *J. Mol. Biol.* **2006**, *361*, 983–992.
- (27) Shimizu, S.; Matubayasi, N. Preferential hydration of proteins: A Kirkwood–Buff approach. *Chem. Phys. Lett.* **2006**, *420*, 518–522.
- (28) Smith, P. E. Chemical potential derivatives and preferential interaction parameters in biological systems from Kirkwood–Buff theory. *Biophys. J.* **2006**, *91*, 849–856.
- (29) Rösgen, J.; Pettitt, B. M.; Bolen, D. W. An analysis of the molecular origin of osmolyte-dependent protein stability. *Protein Sci.* **2007**, *16*, 733–743.
- (30) Holthausen, L. M.; Bolen, D. W. Mixed osmolytes: The degree to which one osmolyte affects the protein stabilizing ability of another. *Protein Sci.* **2007**, *16*, 293–298.
- (31) Kang, M.; Smith, P. Preferential interaction parameters in biological systems by Kirkwood–Buff theory and computer simulation. *Fluid Phase Equilib.* **2007**, *256*, 14–19.

- (32) Hua, L.; Zhou, R.; Thirumalai, D.; Berne, B. Urea denaturation by stronger dispersion interactions with proteins than water implies a 2-stage unfolding. *Proc. Natl. Acad. Sci. U.S.A.* **2008**, *105*, 16928–16933.
- (33) Pierce, V.; Kang, M.; Aburi, M.; Weerasinghe, S.; Smith, P. Recent applications of Birkwood-Buff theory to biological systems. *Cell Biochem. Biophys.* **2008**, *50*, 1–22.
- (34) Auton, M.; Bolen, D.; Rösgen, J. Structural thermodynamics of protein preferential solvation: Osmolyte solvation of proteins, aminoacids, and peptides. *Proteins* **2008**, *73*, 802–813.
- (35) O'Brien, E. P.; Brooks, B.; Thirumalai, D. Molecular origin of constant  $m$ -values, denatured state collapse, and residue-dependent transition midpoints in globular proteins. *Biochemistry* **2009**, *48*, 3743–3754.
- (36) Ghosh, K.; Dill, K. Computing protein stabilities from their chain lengths. *Proc. Natl. Acad. Sci. U.S.A.* **2009**, *106*, 10649–10654.
- (37) Lee, S.; Shek, Y.; Chalikian, T. Urea interactions with protein groups: A volumetric study. *Biopolymers* **2010**, *93*, 866–879.
- (38) Guinn, E.; Pegram, L.; Capp, M.; Pollock, M.; Record, M. J. Quantifying why urea is a protein denaturant, whereas glycine betaine is a protein stabilizer. *Proc. Natl. Acad. Sci. U.S.A.* **2011**, *108*, 16932–16937.
- (39) Cho, S.; Reddy, G.; Straub, J.; Thirumalai, D. Entropic stabilization of proteins by TMAO. *J. Phys. Chem. B* **2011**, *115*, 13401–13407.
- (40) Rösgen, J.; Jackson-Atogi, R. Volume exclusion and H-bonding dominate the thermodynamics and solvation of trimethylamine- $N$ -oxide in aqueous urea. *J. Am. Chem. Soc.* **2012**, *134*, 3590–3597.
- (41) Diehl, R.; Guinn, E.; Capp, M.; Tsodikov, O.; Record, M. J. Quantifying additive interactions of the osmolyte proline with individual functional groups of proteins: Comparisons with urea and glycine betaine, interpretation of  $m$ -values. *Biochemistry* **2013**, *52*, 5997–6010.
- (42) Shek, Y.; Chalikian, T. Interactions of glycine betaine with proteins: Insights from volume and compressibility measurements. *Biochemistry* **2013**, *52*, 672–680.
- (43) Moeser, B.; Horinek, D. Unified description of urea denaturation: Backbone and side chains contribute equally in the transfer model. *J. Phys. Chem. B* **2014**, *118*, 107–114.
- (44) Shimizu, S.; Matubayasi, N. Preferential solvation: Dividing surface vs excess numbers. *J. Phys. Chem. B* **2014**, *118*, 3922–3930.
- (45) Burg, M.; Ferraris, J. Intracellular organic osmolytes: Function and regulation. *J. Biol. Chem.* **2008**, *283*, 7309–7313.
- (46) Garcia-Perez, A.; Burg, M. B. Renal medullary organic osmolytes. *Physiol. Rev.* **1991**, *71*, 1081–1115.
- (47) Jackson-Atogi, R.; Sinha, P.; Rosgen, J. Distinctive solvation patterns make renal osmolytes diverse. *Biophys. J.* **2013**, *105*, 2166–2174.
- (48) Mukaiyama, A.; Koga, Y.; Takano, K.; Kanaya, S. Osmolyte effect on the stability and folding of a hyperthermophilic protein. *Proteins* **2008**, *71*, 110–118.
- (49) Poddar, N.; Ansari, Z.; Singh, R.; Moosavi-Movahedi, A. A.; Ahmad, F. Effect of monomeric and oligomeric sugar osmolytes on deltagd, the gibbs energy of stabilization of the protein at different ph values: Is the sum effect of monosaccharide individually additive in a mixture? *Biophys. Chem.* **2008**, *138*, 120–129.
- (50) Holthauzen, L.; Auton, M.; Sinev, M.; Rösgen, J. Protein stability in the presence of cosolutes. *Methods Enzymol.* **2011**, *492C*, 61–125.
- (51) Yancey, P.; Burg, M. Distribution of major organic osmolytes in rabbit kidneys in diuresis and antidiuresis. *Am. J. Physiol.* **1989**, *257*, F602–7.
- (52) Macmillen, R.; Lee, A. Australian desert mice: Independence of exogenous water. *Science* **1967**, *158*, 383–385.
- (53) Kirkwood, J. G.; Buff, F. P. The statistical mechanical theory of solutions. I. *J. Chem. Phys.* **1951**, *19*, 774–777.
- (54) Ben-Naim, A. Theory of preferential solvation of non-electrolytes. *Cell Biophys.* **1988**, *12*, 255–269.
- (55) Anderson, C. F.; Courtenay, E. S.; Record, M. T. Thermodynamic expressions relating different types of preferential interaction coefficients in solutions containing two solute components. *J. Phys. Chem. B* **2002**, *106*, 418–433.
- (56) Smith, P. E. Equilibrium dialysis data and the relationships between preferential interaction parameters for biological systems in terms of Kirkwood-Buff integrals. *J. Phys. Chem. B* **2006**, *110*, 2862–2868.
- (57) Karunaweera, S.; Gee, M.; Weerasinghe, S.; Smith, P. Theory and simulation of multicomponent osmotic systems. *J. Chem. Theory Comput.* **2012**, *8*, 3493–3503.
- (58) Rösgen, J. Molecular basis of osmolyte effects on protein and metabolites. *Methods Enzymol.* **2007**, *428*, 459–486.
- (59) Santoro, M.; Bolen, D. Unfolding free energy changes determined by the linear extrapolation method. 1. Unfolding of phenylmethanesulfonyl  $\alpha$ -chymotrypsin using different denaturants. *Biochemistry* **1988**, *27*, 8063–8068.
- (60) Makhatadze, G. I. Thermodynamics of protein interactions with urea and guanidinium hydrochloride. *J. Phys. Chem. B* **1999**, *103*, 4781–4785.
- (61) Timasheff, S.; Xie, G. Preferential interactions of urea with lysozyme and their linkage to protein denaturation. *Biophys. Chem.* **2003**, *105*, 421–448.
- (62) Ferreon, A.; Bolen, D. Thermodynamics of denaturant-induced unfolding of a protein that exhibits variable two-state denaturation. *Biochemistry* **2004**, *43*, 13357–13369.
- (63) Mello, C.; Barrick, D. Measuring the stability of partly folded proteins using TMAO. *Protein Sci.* **2003**, *12*, 1522–1529.
- (64) Santoro, M.; Liu, Y.; Khan, S.; Hou, L.; Bolen, D. Increased thermal stability of proteins in the presence of naturally occurring osmolytes. *Biochemistry* **1992**, *31*, 5278–5283.
- (65) Auton, M.; Rösgen, J.; Sinev, M.; Holthauzen, L.; Bolen, D. Osmolyte effects on protein stability and solubility: A balancing act between backbone and side-chains. *Biophys. Chem.* **2011**, *159*, 90–99.
- (66) Vitalis, A.; Pappu, R. ABSINTH: A new continuum solvation model for simulations of polypeptides in aqueous solutions. *J. Comput. Chem.* **2009**, *30*, 673–699.
- (67) Ellison, W. J.; Lamkaouchi, K.; Moreau, J. M. Water: A dielectric reference. *J. Mol. Liq.* **1996**, *68*, 171–279.
- (68) Koradi, R.; Billeter, M.; Wuthrich, K. MOLMOL: A program for display and analysis of macromolecular structures. *J. Mol. Graphics* **1996**, *14*, 51–55.
- (69) Davis-Searles, P. R.; Saunders, A.; Erie, D.; Winzor, D.; Pielak, G. Interpreting the effects of small uncharged solutes on protein-folding equilibria. *Annu. Rev. Biophys. Biomol. Struct.* **2001**, *30*, 271–306.
- (70) Pettersen, E.; Goddard, T.; Huang, C.; Couch, G.; Greenblatt, D.; Meng, E.; Ferrin, T. UCSF chimera—a visualization system for exploratory research and analysis. *J. Comput. Chem.* **2004**, *25*, 1605–1612.
- (71) Auton, M.; Bolen, D. W. Application of the transfer model to understand how naturally occurring osmolytes affect protein stability. *Methods Enzymol.* **2007**, *428*, 397–418.
- (72) Matteoli, E.; Lepori, L. Solute solute interactions in water. 2. An analysis through the Kirkwood-Buff integrals for 14 organic solutes. *J. Chem. Phys.* **1984**, *80*, 2856–2863.
- (73) Rösgen, J.; Hinz, H. Response functions of proteins. *Biophys. Chem.* **2000**, *83*, 61–71.
- (74) Royer, C. Revisiting volume changes in pressure-induced protein unfolding. *Biochim. Biophys. Acta, Protein Struct. Mol. Enzymol.* **2002**, *1595*, 201–209.
- (75) Lin, L.; Brandts, J.; Brandts, J.; Plotnikov, V. Determination of the volumetric properties of proteins and other solutes using pressure perturbation calorimetry. *Anal. Biochem.* **2002**, *302*, 144–160.
- (76) Ravindra, R.; Winter, R. Pressure perturbation calorimetric studies of the solvation properties and the thermal unfolding of proteins in solution. *Z. Phys. Chem.* **2003**, *217*, 1221–1243.

(77) Kokubo, H.; Hu, C.; Pettitt, B. Peptide conformational preferences in osmolyte solutions: Transfer free energies of decaalanine. *J. Am. Chem. Soc.* **2011**, *133*, 1849–1858.

(78) Qu, Y.; Bolen, C.; Bolen, D. Osmolyte-driven contraction of a random coil protein. *Proc. Natl. Acad. Sci. U.S.A.* **1998**, *95*, 9268–9273.

(79) Holthauzen, L.; Rösgen, J.; Bolen, D. Hydrogen bonding progressively strengthens upon transfer of the protein urea-denatured state to water and protecting osmolytes. *Biochemistry* **2010**, *49*, 1310–1318.

(80) Sosnick, T.; Mayne, L.; Englander, S. Molecular collapse: The rate-limiting step in two-state cytochrome c folding. *Proteins* **1996**, *24*, 413–426.

(81) Baskakov, I.; Bolen, D. Monitoring the sizes of denatured ensembles of staphylococcal nuclease proteins: Implications regarding  $m$  values, intermediates, and thermodynamics. *Biochemistry* **1998**, *37*, 18010–18017.

(82) Tran, H.; Mao, A.; Pappu, R. Role of backbone-solvent interactions in determining conformational equilibria of intrinsically disordered proteins. *J. Am. Chem. Soc.* **2008**, *130*, 7380–7392.

(83) Ziv, G.; Thirumalai, D.; Haran, G. Collapse transition in proteins. *Phys. Chem. Chem. Phys.* **2009**, *11*, 83–93.

(84) Konuma, T.; Kimura, T.; Matsumoto, S.; Goto, Y.; Fujisawa, T.; Fersht, A.; Takahashi, S. Time-resolved small-angle X-ray scattering study of the folding dynamics of barnase. *J. Mol. Biol.* **2011**, *405*, 1284–1294.

(85) Yoo, T.; Meisburger, S.; Hinshaw, J.; Pollack, L.; Haran, G.; Sosnick, T.; Plaxco, K. Small-angle X-ray scattering and single-molecule fret spectroscopy produce highly divergent views of the low-denaturant unfolded state. *J. Mol. Biol.* **2012**, *418*, 226–236.

(86) Hu, C.; Kokubo, H.; Lynch, G.; Bolen, D.; Pettitt, B. Backbone additivity in the transfer model of protein solvation. *Protein Sci.* **2010**, *19*, 1011–1022.

(87) Ferreon, A. C.; Ferreon, J. C.; Bolen, D. W.; Rösgen, J. Protein phase diagrams II: Nonideal behavior of biochemical reactions in the presence of osmolytes. *Biophys. J.* **2007**, *92*, 245–256.

(88) Gulotta, M.; Qiu, L.; Desamero, R.; Rösgen, J.; Bolen, D.; Callender, R. Effects of cell volume regulating osmolytes on glycerol 3-phosphate binding to triosephosphate isomerase. *Biochemistry* **2007**, *46*, 10055–10062.

(89) Duff, M. J.; Grubbs, J.; Serpersu, E.; Howell, E. Weak interactions between folate and osmolytes in solution. *Biochemistry* **2012**, *51*, 2309–2318.